Mon. Not. R. Astron. Soc. **000**, 1–8 (YYYY) Printed 1 February 2008 (MN LATEX style file v2.2)

Radio emission from the Sy 1.5 galaxy NGC 5033

M. A. Pérez-Torres[1⋆] and A. Alberdi[1]
[1] *Instituto de Astrofísica de Andalucía, CSIC, Apdo. Correos 3004, E-18080 Granada, Spain*

Accepted 2007 May 4. Received 2007 May 2; in original form 2007 March 23

ABSTRACT

We present new continuum VLA observations of the nearby Sy 1.5 galaxy NGC 5033, made at 4.9 and 8.4 GHz on 8 April 2003. Combined with VLA archival observations at 1.4 and 4.9 GHz made on 7 August 1993, 29 August 1999, and 31 October 1999, we sample the galaxy radio emission at scales ranging from the nuclear regions ($\lesssim 100$ pc) to the outer regions of the disk (~ 40 kpc). The high-resolution VLA images show a core-jet structure for the Sy 1.5 nucleus. While the core has a moderately steep non-thermal radio spectrum ($S_\nu \propto \nu^\alpha; \alpha_{1.5}^{4.9} \approx -0.4$), the inner kpc region shows a steeper spectrum ($\alpha_{1.5}^{8.4} \approx -0.9$). This latter spectrum is typical of galaxies where energy losses are high, indicating that the escape rate of cosmic ray electrons in NGC 5033 is low. The nucleus contributes little to the total 1.4 GHz radio power of NGC 5033 and, based on the radio to far-infrared (FIR) relation, it appears that the radio and far-infrared emission from NGC 5033 are dominated by a starburst that during the last 10 Myr produced stars at a rate of $2.8\,\mathrm{M}_\odot\,\mathrm{yr}^{-1}$ yielding a supernova (type Ib/c and II) rate of $0.045\,\mathrm{yr}^{-1}$. This supernova rate corresponds to about 1 SN event every 22 yr. Finally, from our deep 8.4 GHz VLA-D image, we suggest the existence of a radio spur in NGC 5033, which could have been due to a hot superbubble formed as a consequence of sequential supernova explosions occurring during the lifetime of a giant molecular cloud.

Key words: Galaxies: individual: NGC 5033 - Galaxies: Seyfert, starburst - Radio continuum: general – Radiation mechanisms: non-thermal

1 INTRODUCTION

Radio emission from normal galaxies is dominated by synchrotron emission from relativistic cosmic ray electrons (CRE) at low frequencies ($\lesssim 30$ GHz), while at high frequencies ($\nu \gtrsim 30$ GHz) the dominant emitting mechanism is thermal free-free emission from ionized gas at temperatures of $\sim 10^4$ K.

With the advent of the Infrared Astronomical Satellite (IRAS, Neugebauer et al. 1984), a sample of $\approx 20,000$ galaxies complete to 0.5 Jy in the 60 μm band was detected, the majority of which had not been previously cataloged. While the observed FIR luminosity from most of those galaxies can be explained by ongoing star formation and starburst activity, some of the most luminous infrared galaxies may host an active galactic nucleus (AGN). Nearly all of the radio emission at wavelengths longer than a few cm from such galaxies is synchrotron radiation from relativistic electrons and free-free emission from H II regions. In turn, this synchrotron radio emission is a direct probe of the recent massive starforming activity, since only stars more massive than about $8\mathrm{M}_\odot$result in the Type Ib/c and II supernovae, which are thought to accelerate most of the relativistic electrons that are responsible for the observed synchrotron radio emission. This results in an extremely good correlation between radio and far-infrared emission among galaxies (e.g., Harwit & Pacini 1975, Condon et al. 1991a, Condon et al. 1991b). If an AGN is present, then the associated radio continuum, in excess of the level expected from the star formation, may be detected and, by means of high-resolution observations, its contribution to the total radio emission subtracted.

Synchrotron radio emission also carries relevant information on the magnetic field and the particle feeding, or re-acceleration mechanisms present in galaxies. Since the synchrotron energy loss rate of relativistic electrons, dE/dt, varies with the particle energy squared, E^2, the typical lifetime of a relativistic electron, subject to radiative synchrotron losses is $t_{\rm syn} = E/(dE/dt) \propto E^{-1}$. Further, the critical frequency at which an electron radiates most of its synchrotron emission is $\nu_{\rm c} \propto E^2$, and hence $dE/dt \propto \nu_{\rm c}$, and $t_{\rm syn} \propto \nu_{\rm c}^{-1/2}$. Therefore, regions with little ongoing relativistic particle re-supply, or re-acceleration have steeper synchrotron spectra, which may be revealed by

⋆ E-mail:torres@iaa.es (MAPT); antxon@iaa.es (AA)

multi-frequency radio interferometry observations. The sites and length scales where the spectral evolution is happening can also be revealed by high-resolution radio interferometry observations, which tell us where CRE are accelerated.

High-resolution radio observations also allow the detailed study of both thermal and non-thermal emission in nearby, normal galaxies (e.g. Condon 1992). Those observations are needed, as the spatially integrated nonthermal spectral index is in general a poor diagnostic for the type of propagation or the importance of energy losses. On the contrary, spatially resolved radio data for the haloes of galaxies allow us to draw firm conclusions. For example, the steepening of the spectrum away from the disk is an indication that synchrotron and inverse Compton losses are taking place during the propagation of cosmic ray electrons in the halo (Lisenfeld & Voelk 2000).

NGC 5033 is a nearby (D=13 Mpc) spiral galaxy that exhibits strong CO emission out to at least $R \sim 50\farcm$, and contains a Seyfert 1.5 nucleus (Ho et al. 1997). NGC 5033 also displays strong far infrared luminosity ($L_{[8-1000\mu\ \mathrm{m}]} = 1.20 \times 10^{10} \mathrm{L}_{\odot}$; Sanders et al. 2003), and has been host to at least three supernovae in the last 60 yr (SN 1950C, SN 1985L, and SN 2001gd). Here, we present and discuss continuum VLA-D observations of NGC 5033 at 1.4, 4.9 and 8.4 GHz taken on April 8, 2003, complemented with archival VLA data taken on August 29, 1999 (1.4 GHz, A-configuration) and October 31, 1999 (4.9 GHz, B-configuration), respectively. The resolutions yielded by the different arrays and frequencies allow us to trace the synchrotron emission not only in the innermost regions of the galaxy, but also in the inner and outer disk, and the galactic halo.

The paper is organized as follows: we report on the radio observations in Sect. 2; we present our results in Sect. 3 and discuss them in Sect. 4. We summarize our main conclusions in Sect. 5. We assume throughout the paper a distance of 13 Mpc to the host galaxy of SN 2001gd, NGC 5033, based on its redshift ($z = 0.002839$; Falco et al. 1997) and assumed values of $H_0 = 65\,\mathrm{km\ s^{-1}\ Mpc^{-1}}$ and q_0=0. At the distance of NGC 5033 $1''$ corresponds to a linear size of 64 pc.

2 OBSERVATIONS

We reanalysed archival VLA data on NGC 5033 obtained under program AU0079 on 1999 August 29 (1.4 GHz, A-configuration) and 1999 October 31 (4.9 GHz, B-configuration), respectively. These data sets provide very similar angular resolution, since the increase in angular resolution from 1.4 to 4.9 GHz is essentially compensated by a decrease in the longest antenna separation, which is approximately a factor of three between the A and B configurations of the VLA. In both observing epochs, the VLA recorded both senses of circular polarization. Each frequency band was split into two intermediate frequencies (IFs), of 50 MHz bandwidth each. 3C 286 was used to set the absolute VLA flux density scale, and J1310+323 was used as the phase calibrator at both frequencies.

We also show unpublished archival 1.4 GHz continuum VLA data obtained under program AP270 on 1993 August 7, when the VLA was in C-configuration. The VLA recorded only the left sense of circular polarization, and the observations were made in spectral line mode, since the aim was to image the 21-cm hydrogen line emission of NGC 5033. The 6.2-MHz IF at 1.4 GHz was split into 63 spectral channels, each of 97.66 kHz bandwidth. For the purposes of imaging the continuum radio emission at 1.4 GHz, we used the channel-0 data, which contains the inner 75% of the line data. 3C 286 was used to set the absolute VLA flux density scale, and the source 1323+321 was used as the phase calibrator. While the total synthesized bandwidth was small, the large time on-source (about 5.5 hr) and excellent uv-coverage allowed us to obtain the deepest 21 cm image ever of the Sy 1.5 galaxy NGC 5033 (see top left panel in Fig. 1).

Finally, we show observations at 4.9 and 8.4 GHz of SN 2001gd and its host galaxy NGC 5033, made on 2003 April 8 with the VLA in D-configuration, as part of our VLBI observing program to monitor the angular expansion of SN 2001gd (Pérez-Torres et al 2005). The VLA recorded both senses of circular polarization, and each frequency band was split into two intermediate frequencies (IFs), of 50 MHz bandwidth each. We used 3C 286 to set the absolute VLA flux density scale at both frequencies. We used J1310+323 as the phase calibrator at 4.9 GHz, while J1317+34 was used as the phase calibrator at 8.4 GHz.

For all data sets, we used standard calibration and hybrid mapping techniques within the Astronomical Image Processing System (*AIPS*) to obtain the images shown in Figure 1.

3 RESULTS

Figure 1 and Table 1 summarize our results for the total intensity radio images of NGC 5033, obtained with the VLA. The flux density errors given for the VLA measurements in Table 1 represent one statistical standard deviation, and are a combination of the off-source rms in the image and a fractional error, ϵ, included to account for the inaccuracy of VLA flux density calibration and possible deviations of the primary calibrator from an absolute flux density scale. The final errors, σ_f, as listed in Table 1, are taken as $\sigma_f^2 = (\epsilon\, S_0)^2 + \sigma_0^2$ where S_0 is the measured flux density, σ_0 is the off-source rms at a given frequency, and ϵ=0.05 at 1.4 GHz, and 0.02 at 4.9 GHz and 8.4 GHz, respectively. We note that the total quoted flux density errors are dominated by the uncertainties in the VLA calibration (ϵ). The positions of the peaks of brightness for all the VLA images coincide among them within the errors, and correspond to the nucleus of NGC 5033.

The 1.4 GHz VLA-C image (panel a in Fig. 1) shows the whole disk of NGC 5033, with an angular size of about $10' \times 5'$ ($\simeq$ 38 kpc $\times$ 19 kpc). The low-surface brightness, extended emission clearly follows the optical emission from the spiral arms of the galaxy, and most of the local maxima of both optical and radio emission are spatially coincident with H II regions (Evans 1996). The total flux density above the lowest drawn contour is about 355 mJy, of which $\sim$58 mJy are within a circumnuclear region of $30'' \times 30''$($\approx 1.8 \times 1.8$ kpc^2). We also detected three strong sources embedded within the extended 1.4 GHz emission of the disk, which we dubbed N1, SW1, and SW2 in panels (a) and (f), and whose nature is discussed in section 4.

The extension of the 4.9 GHz VLA-D total intensity

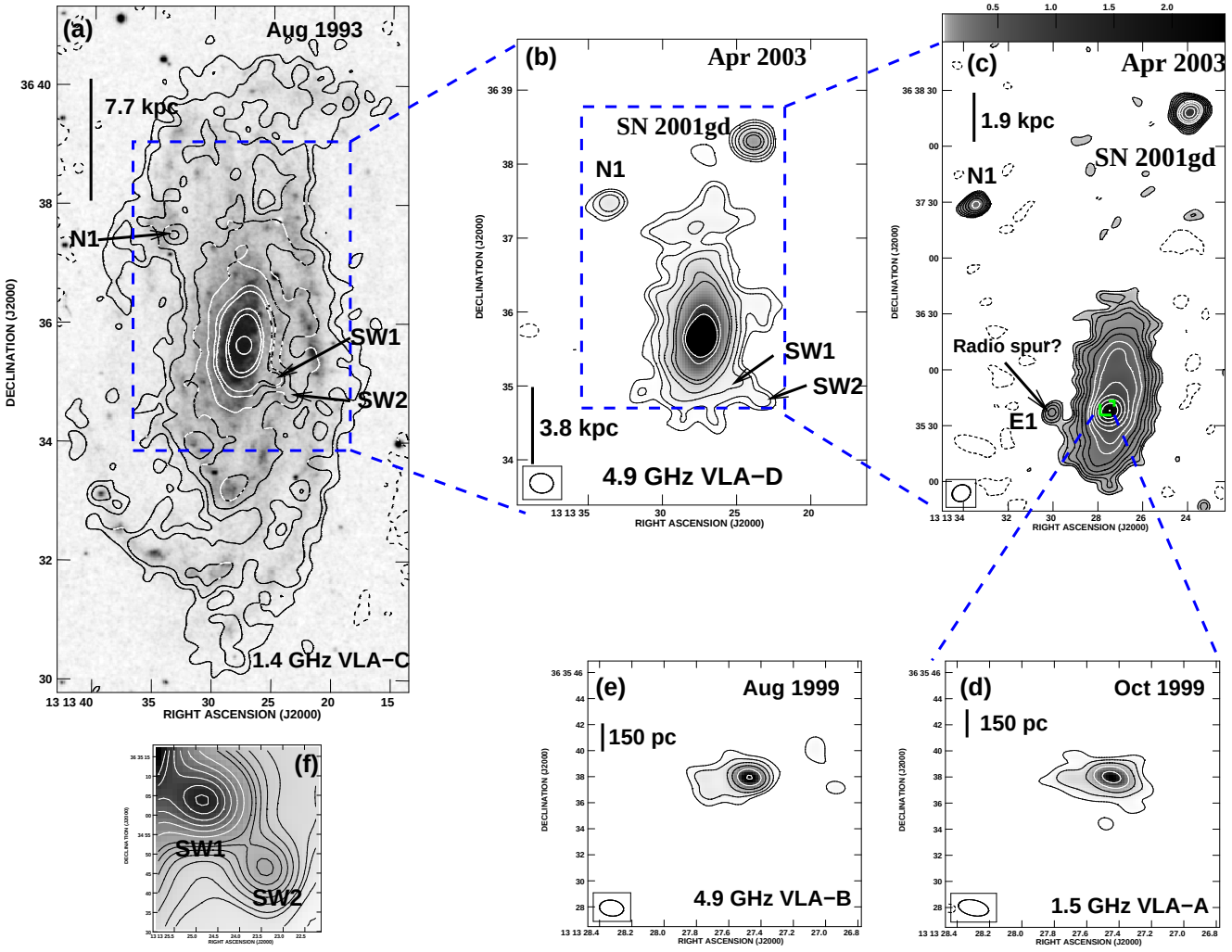

Figure 1. **(a)** Contours of 1.4 GHz observations made on 7 August 1993 with the VLA-C, overlaid on a Digitized Sky Survey (DDS2) Blue plate of NGC 5033; **(b,c)** total intensity radio images of NGC 5033 obtained from 4.9 and 8.4 GHz VLA-D observations on 8 April 2003; **(d,e)** 1.4 GHz VLA-A observations on 29 August 1999 and 4.9 GHz VLA-B observations on 31 October 1999; **(f)** blow-up of the 1.4 GHz VLA-C image, around the SW1 and SW2 regions. VLA contours are drawn at (-3,3,3$\sqrt{2}$,9,...)$\times$ the off-source rms of each map, which are of 93 μJy beam^{-1} (1.4 GHz VLA-C), 45 μJy beam^{-1} (4.9 GHz VLA-D), 19 μJy beam^{-1} (8.4 GHz VLA-D), and of 170 and 70 μJy beam^{-1} at 1.4 and 4.9 GHz (panels d and e), respectively. The peaks of brightness are of 31.8, 10.6, and 2.4 mJy beam^{-1} at 1.4, 4.9, and 8.4 GHz (top panels), and of 5.7 and 3.4 mJy beam^{-1} at 1.5 and 4.9 GHz (panels d and e). The principal dimensions (major axis $\times$ minor axis, position angle) of the restoring beams are: 17.″3 $\times$15.″4, 83°(a); 19.″1 $\times$15.″9, 83°(b); 10.″1 $\times$8.″7, -61°(c); 2.″3 $\times$1.″2, 78°(d); 1.″8 $\times$1.″2, 82°(e).

emission of NGC 5033 (panel b) is about $230'' \times 130''$($\simeq$ 14.7 kpc$\times$ 8.3 kpc), significantly smaller than the 1.4 GHz radio emitting region. Since the 1.4 GHz VLA-C observations have a very similar resolution to our 4.9 GHz VLA-D observations, this finding indicates that the external regions of the disk are partially resolved at this frequency. The total flux density of the nuclear regions of NGC 5033 above the lowest drawn contour is $\simeq$45.3 mJy. Note also that the extended galactic emission at 4.9 GHz around SN 2001gd is resolved out. Note that there is no contamination of background synchrotron emission around the position of SN 2001gd, which is clearly detected at 4.9 GHz. We note that N1, SW1, and SW2 are also detected at this frequency, despite the 10 years elapsed between the 1.4 and 4.9 GHz VLA observations.

The extension of the 8.4 GHz VLA-D emission from the nuclear regions of NGC 5033 (panel c) is about $110'' \times 50''$($\simeq$ 6.9 kpc $\times$ 3.2 kpc), a size similar to that of the 4.9 GHz radio emitting region. The total flux density for the nuclear region of NGC 5033 above the lowest drawn contour is $\simeq$11.7 mJy. Note that component N1, as well as the supernova SN 2001gd, are clearly detected outside the main bulk of the nuclear radio emitting region. Note also that a new component, E1, is detected close to the inner regions of the disk, while components SW1 and SW2 are not detected above a limiting flux density of 57μJy/b

Panels (d) and (e) of Fig. 1 correspond to radio images of the nuclear regions of NGC 5033, obtained at 1.5 and 4.9 GHz from archival observations made with the VLA in A- and B-configuration, respectively. The peaks of brightness are of 5.7 and 3.4 mJy beam^{-1} at 1.5 and 4.9 GHz,

Table 1. VLA sources within the galaxy NGC 5033

Source	$\alpha(J2000.0)$	$\delta(J2000.0)$	$S^P_{1.4}$ (mJy/b)	$S^I_{1.4}$ (mJy)	$S^P_{4.9}$ (mJy/b)	$S^I_{4.9}$ (mJy)	$S^P_{8.4}$ (mJy/b)	$S^I_{8.4}$ (mJy)
NGC 5033∗†	$13^h13^m27\overset{s}{.}4430$	$36°35'37\overset{''}{.}880$	5.7 ± 0.15	12.73 ± 0.30	3.83 ± 0.02	6.25 ± 0.33	···	···
NGC 5033‡	···	···	31.9 ± 0.09	355.41 ± 1.64	10.6 ± 0.03	45.46 ± 0.23	2.4 ± 0.02	11.72 ± 0.12
N1[a]	$13^h13^m33\overset{s}{.}4517$	$36°37'29\overset{''}{.}116$	1.63 ± 0.09	3.01 ± 0.24	0.66 ± 0.03	0.70 ± 0.05	0.36 ± 0.02	0.29 ± 0.02
SW1[a]	$13^h13^m24\overset{s}{.}862$	$36°35'04\overset{''}{.}48$	4.46 ± 0.09	9.44 ± 0.28	0.47 ± 0.03	2.17 ± 0.15	···	···
SW2[b]	$13^h13^m23\overset{s}{.}995$	$36°34'38\overset{''}{.}95$	1.85 ± 0.09	4.33 ± 0.29	0.32 ± 0.03	0.53 ± 0.07	···	···
E1[a]	$13^h13^m30\overset{s}{.}435$	$36°35'37\overset{''}{.}130$	···	···	···	···	0.12 ± 0.02	0.12 ± 0.02

† The coordinates correspond to the putative nucleus of NGC 5033, dubbed NGC 5033*, as seen with the VLA-A and VLA-B at 1.4 GHz (October 1999) and 4.9 GHz (August 199), respectively. S^P_ν and S^I_ν are the peak and integrated flux densities for each given component, at a frequency ν. ‡ Peak and integrated flux densities for NGC 5033, as seen with the VLA-C and VLA-D at 1.4 (August 1993), 4.9 (April 2003), and 8.4 GHz (April 2003). [a] Source tentatively identified as background source by Ho & Ulvestad (2001); [b] Source position coincident with an H II region (Evans 1996).

respectively, and correspond to the emission from the core. A jet pointing eastwards from the core is also seen at both frequencies. The different position angle of the jet, as obtained at 1.4 GHz with respect to 5.0 GHz cannot be fully accounted for by the different synthesized beam at each of the two frequencies. In fact, while the 1.4 GHz VLA data displays a very well collimated jet, the 4.9 GHz VLA data shows a hint for a double-layer jet structure, which is very suggestive of the spine/shear layer model proposed by Laing & Brid (2002) to explain the synchrotron radio emission of Fanaroff-Riley radio galaxies. We also note that, while the position angle of the upper layer of the 4.9 GHz jet coincides well with that seen at 1.4 GHz, the bottom layer of the 4.9 GHz jet is not seen at 1.4 GHz. This could point to opacity effects at the base of the jet playing a relevant role, which could be responsible for shaping the position angles seen at 1.4 and 4.9 GHz.

3.1 Background sources

We obtained the 1.4 GHz VLA-C image in Fig. 1 (panel a) by using wide-field techniques, to accurately take into account the contribution to the total radio emission from confusing sources within an area of $50' \times 50'$ around the nucleus of NGC 5033. We used the AIPS task SAD to search for point-like sources above a flux density level cutoff of five times the off-source (1 rms=93 μJy beam^{-1}). This resulted in the detection of a total of 49 background sources (i.e., outside the lowest drawn contour in panel (a) of Fig. 1), detected above five times the off-source rms (1 rms = 93 μJy beam^{-1}). In Table 2, we list the coordinates, peak, and integrated flux densities for each source component detected at 1.4 GHz. A number of sources exist in the literature (see caption of Table 2), but many of them are detected for the first time. The most striking finding among these background sources is B2 1312+36 (Colla et al. 1973), which showed a peak flux density of 226.1 mJy beam^{-1}on 7 August 1993, and of 4.6 mJy beam^{-1}at 4.9 GHz on 8 April 2003. The enormous difference in flux density between the two frequencies would imply an ultra steep spectrum for B2 1312+36. However, the non-simultaneity of these observations do not allow for a precise estimate of α. Fortunately, we were able to make use of snapshot 1.4 GHz VLA observations taken also on 8 April 2003, to precisely determine α. The 1.4 GHz peak flux density of B2 1312+36 was of 190.3 mJy beam^{-1}, indicating $\alpha^{4.9}_{1.4} = -3.1 \pm 0.1$ ($S_\nu \propto \nu^\alpha$), and thus confirming that B2 1312+36 is an ultra steep spectrum (USS) source. Such steep spectrum is found either in pulsars, or in very variables sources (e.g. De Breuck et al. 2000, Izvekova et al. 1981). A FIRST image of B2 1312+36, taken on 17 July 1994, shows a 1.4 GHz peak flux density of 438.6 mJy/b, which confirms this source displays strong flux density variations, and hence is very unlikely to be a pulsar. The source has no optical counterpart at the limit of the POSS I plates ($m_R \approx$20.0) and SDSS plates ($m_v \approx$24.0), neither an infrared counterpart at the limit of the 2MASS plates (J≈15.8; H≈15.1; K≈14.3).

4 DISCUSSION

4.1 The radio spectrum and magnetic field of NGC 5033

We used the VLA archival data obtained in 1999 under project AU0079 to derive the spectral index of the core-jet structure that is seen in panels (d) and (e) of Figure 1. Since the angular resolution of the 4.9 GHz VLA observations in A-configuration is essentially the same achieved by the 1.5 Ghz VLA observations in B-configuration, we used the peaks of brightness at each frequency (as given by the AIPS task IMSTAT) to estimate the spectral index of the compact, nuclear source. We obtained $\alpha = 0.44 \pm 0.04$, which is in agreement with the spectral index published by Ho & Ulvestad (2001) and confirms the AGN-like nature of the radio emission from the nuclear region of this Sy 1.5 galaxy. Since the angular resolution of the 4.9 GHz VLA-D is very close to that of the 1.4 GHz VLA-C, we can estimate the spectral index of the kiloparsec scale disk of NGC 5033. Using the peaks of brightness at those frequencies, we obtain $\alpha = -0.93 \pm 0.02 (S_\nu \propto \nu^\alpha$, indicating an steep synchrotron spectral index of the radio emission within the inner few kiloparsecs of NGC 5033. Lisenfeld & Voelk 2000 have shown that galaxies having steep spectral radio indices ($\alpha \lesssim -0.9$) with increasing distance from the disk tend to have significant inverse Compton and synchrotron energy losses of cosmic ray electrons, indicating that their escape rate is low (e.g., M 82 (Seaquist & Odegard 1991); NGC 253 (Carilli et al. 1992); NGC 2146 (Lisenfeld et al.

Table 2. 1.4 GHz Background sources†

$\alpha(J2000.0)$	$\delta(J2000.0)$	$S^P_{1.4}$ (mJy/b)	$S^I_{1.4}$ (mJy)
$13^h11^m38^s.347$	$36°41'22''.20$	0.73	0.74
$13^h11^m46^s.609$	$36°20'12''.49$	3.29	4.45
$13^h11^m48^s.016$	$36°19'57''.67$	[1]4.77	7.06
$13^h11^m55^s.739$	$36°36'06''.44$	0.57	0.59
$13^h12^m04^s.680$	$36°23'18''.17$	[2]15.27	15.87
$13^h12^m12^s.688$	$36°13'13''.92$	4.70	7.55
$13^h12^m14^s.370$	$36°49'01''.94$	1.15	1.25
$13^h12^m15^s.339$	$36°18'01''.52$	1.08	1.39
$13^h12^m24^s.732$	$36°40'51''.28$	6.54	7.32
$13^h12^m25^s.069$	$36°37'27''.05$	[2]2.17	2.29
$13^h12^m25^s.575$	$36°23'45''.68$	0.76	0.92
$13^h12^m25^s.608$	$36°43'26''.39$	0.57	0.61
$13^h12^m26^s.132$	$36°23'21''.07$	1.31	1.61
$13^h12^m26^s.534$	$36°26'25''.30$	0.47	0.37
$13^h12^m33^s.178$	$36°12'55''.26$	1.32	1.65
$13^h12^m34^s.779$	$36°57'18''.14$	0.82	0.91
$13^h12^m37^s.528$	$36°13'57''.09$	0.81	1.55
$13^h12^m40^s.263$	$36°48'29''.27$	0.49	0.77
$13^h12^m51^s.637$	$36°11'05''.08$	0.72	0.87
$13^h12^m57^s.602$	$36°47'42''.15$	0.58	0.61
$13^h13^m00^s.943$	$36°25'06''.26$	0.54	0.64
$13^h13^m01^s.709$	$36°48'33''.70$	0.94	1.31
$13^h13^m01^s.878$	$36°47'40''.72$	1.10	1.24
$13^h13^m02^s.086$	$36°39'43''.77$	1.32	1.88
$13^h13^m03^s.766$	$36°33'29''.96$	5.16	4.71
$13^h13^m04^s.877$	$36°30'05''.62$	0.70	0.55
$13^h13^m10^s.193$	$36°34'42''.07$	[3]4.88	4.17
$13^h13^m15^s.991$	$36°24'46''.22$	3.15	5.14
$13^h13^m16^s.664$	$36°25'06''.13$	1.06	0.76
$13^h13^m19^s.228$	$36°39'40''.95$	0.49	2.57
$13^h13^m22^s.943$	$36°40'05''.27$	0.55	4.87
$13^h13^m23^s.156$	$36°34'41''.93$	1.19	3.08
$13^h13^m23^s.495$	$36°55'24''.94$	2.43	2.47
$13^h13^m27^s.121$	$36°46'03''.38$	0.72	0.48
$13^h13^m39^s.284$	$36°50'20''.10$	[2]2.79	3.28
$13^h13^m49^s.120$	$36°49'26''.25$	0.50	1.09
$13^h13^m57^s.673$	$36°27'40''.99$	0.53	0.52
$13^h14^m07^s.458$	$36°42'08''.60$	0.61	1.02
$13^h14^m08^s.645$	$36°15'43''.77$	1.69	2.08
$13^h14^m09^s.508$	$36°28'54''.98$	0.85	1.35
$13^h14^m17^s.867$	$36°49'14''.62$	[4]15.91	16.20
$13^h14^m29^s.894$	$36°42'55''.64$	3.55	4.20
$13^h14^m30^s.051$	$36°23'29''.51$	0.79	1.15
$13^h14^m39^s.929$	$36°35'04''.09$	0.69	1.10
$13^h14^m42^s.432$	$36°39'24''.84$	0.93	0.74
$13^h14^m43^s.392$	$36°32'18''.47$	2.50	2.65
$13^h14^m44^s.308$	$36°39'02''.59$	[1]226.11	228.37
$13^h15^m25^s.329$	$36°47'13''.79$	1.29	1.90
$13^h15^m28^s.865$	$36°50'08''.62$	0.95	1.80

† Background sources of the 1.4 GHz NGC 5033 field, from VLA observations obtained on 7 August 1993 with the VLA-C. $S^P_{1.4}$ and $S^I_{1.4}$ are the peak and integrated flux densities of each component, respectively. We used the AIPS task SAD to search for point-like sources above a flux density level cutoff of five times the off-source (1 rms=93 μJy beam^{-1}). [1]Colla et al. (1973); [2]McMahon et al. (2002); [3]Ho & Ulvestad (2001); [4]Hales et al. (1988);

1996); NGC 4666 (Sukumar et al. 1988)). While the spectral index we find for the kiloparsec region of NGC 5033 hints to the fact that energy losses are important, we cannot exclude that the observed spectrum is due to a rather normal, relativistic electron energy distribution with $p \approx 2.8$ ($N(E) \propto E^{-p}$).

The 1.4 GHz monochromatic luminosity of the core of NGC 5033, as obtained with the VLA in A-configuration, is equal to of $L_{1.5} = (1.2 \pm 0.2) \times 10^{27}\, D^2_{13}$ ergs s^{-1} Hz^{-1}, and the integrated isotropic radio luminosity between 300 MHz and 30 GHz is, for $\alpha = -0.44$, of $L_{\rm core} = (1.5 \pm 0.2) \times 10^{37}\, D^2_{13}$ ergs s^{-1}. From our VLA observations in D-configuration, we obtain a 1.4 GHz monochromatic luminosity for the nuclear regions of the galaxy NGC 5033 of $L_{1.4} = (3.0 \pm 0.3) \times 10^{28}\, D^2_{13}$ ergs s^{-1} Hz^{-1}. If the spectral index of $\alpha = -0.9$ extends at least from 300 MHz to 30 GHz, then the integrated isotropic radio luminosity for the nuclear regions of the galaxy is $L_{\rm R} = (2.3 \pm 0.2) \times 10^{38}\, D^2_{13}$ ergs s^{-1}. We can then estimate the average magnetic field in the radio emitting regions NGC 5033. Following Pacholczyk (1970), we have

$$B_{\rm min} = (4.5\, c_{12}/\phi)^{2/7}\, (1+\psi)^{2/7}\, R^{-6/7}\, L_{\rm R}^{2/7} \qquad (1)$$

where $L_{\rm R}$ is the radio luminosity of the source, in ergs s^{-1}; R is the characteristic linear size of the source, in cm; c_{12} is a slowly-varying function of the spectral index (Pacholczyk 1970); ϕ is the filling factor of fields and particles, i.e. the ratio of the volume filled with relativistic particles and magnetic fields to the total volume occupied by the source; and ψ is the ratio of the heavy particle energy to the electron energy. Since the value of ϕ is highly uncertain, we will set it to ϕ=0.5 for the sake of simplicity. The value of ψ depends on the mechanism that generates the relativistic electrons, and can range from 1 to 2000. We will adopt here a value of $\psi = 100$, which seems appropriate for galaxies (Moffet 1973). As the characteristic size of the source, R we took an angular region of $30'' \times 30''$centered in the nucleus of NGC 5033, which approximately corresponds to the inner region of the galaxy disk. The corresponding approximate flux density values at each frequency are of 58, 21, and 6 mJy at 1.4, 4.9, and 8.4 GHz. With the above values, Eq. 1 results in minimum magnetic field values of 23, 22, and 18 μG at 1.4, 4.9, and 8.4 GHz, respectively. Therefore, if the situation is close to equipartition, the average magnetic field in the inner region of the disk is of about 20 μG.

4.2 Radio/FIR correlation and the star-formation rate of NGC 5033

The existing linear correlation between the total radio continuum emission and the far-IR luminosity ($L_{\rm FIR}$) is well known in "normal" galaxies (Condon 1992), and is generally interpreted as being due to the presence of massive stars. These massive stars provide relativistic particles via supernova explosions and heat the interstellar dust, which then re-radiates the energy at FIR wavelengths (Helou et al. 1985; Condon 1992). The ratio of infrared to radio luminosity is usually expressed through the q-parameter (Helou et al. 1985), which is defined as $q = \log\,[(FIR/3.75 \times 10^{12})/S_{1.4\ \rm GHz}]$, where $S_{1.4\rm GHz}$ is the observed 1.4 GHz flux density in units of W m^{-2} Hz^{-1}, and FIR is given by $FIR = 1.26 \times 10^{-14}(2.58 S_{60\ \mu\rm m} + S_{100\ \mu\rm m})$ where $S_{60\mu m}$ and

$S_{100\mu m}$ are IRAS 60 μm and 100 μm band flux densities, in Jy (Helou et al. 1988).

Therefore, q is a measure of the logarithmic FIR/radio flux-density ratio, and is an indicator of the relative importance of an AGN, or starburst in a galaxy. Most galaxies in the IRAS Bright Galaxy Sample have $q \approx 2.34$, though some galaxies have smaller q values due to additional contributions from compact radio cores and radio jets/lobes (Sanders & Mirabel 1996). The bulk of the far infra-red emission comes from a region of angular size of radius $30''(\approx 1.9$ kpc), as measured from an archival ISO image of NGC 5033. Hence, to compute q, we estimated the 1.4 GHz radio emission from a circumnuclear region of the same angular size, using the AIPS task JMFIT. The resulting value is of about 58 mJy, which translates into an isotropic luminosity of $L_{1.4} = 1.2 \times 10^{21}$ W Hz^{-1}. The IR flux densities at 60 and 100 μm are $S_{60\ \mu\mathrm{m}} = 16.20$ Jy and $S_{100\ \mu\mathrm{m}} = 50.23$ Jy, respectively (Sanders et al. 2003). The resulting q-parameter -after subtraction of the radio emission contributed by the nucleus- is q=2.83. Yun et al. (2001) pointed out that values of q less than 1.64 would indicate the radio dominance of an AGN. Thus, it appears that the radio nucleus of the Sy 1.5 galaxy NGC 5033 is of very low-luminosity, and the radio emission from its circumnuclear region is dominated by starburst activity. We can characterize such a starburst by, e.g., following the prescriptions by Scoville et al. (1997), which characterize a starburst by its total luminosity, L, Ly continuum production, Q, and accumulated stellar mass, $M_\star$. Those values are obtained as power-law approximations of the lower and upper mass cutoffs for stars, m_l and m_u, the constant rate of star formation, $\dot{M}$, and the burst timescale, t_B. In particular, a starburst lasting 10 Myr and producing stars at a rate of $2.8\,\mathrm{M}_\odot\,\mathrm{yr}^{-1}$ in the range $m_l = 1\,\mathrm{M}_\odot$ and $m_u = 40\,\mathrm{M}_\odot$, yields essentially the same observed far-infrared luminosity of NGC 5033 ($L_{\mathrm{FIR}} = 1.2 \times 10^{10}\,\mathrm{L}_\odot$), and results into a Ly continuum production of $Q \approx 3 \times 10^{53}\mathrm{s}^{-1}$, and $M_\star \approx 9 \times 10^7 \mathrm{M}_\odot$. To estimate the supernova rate, we used a minimum mass for yielding Type II supernovae of $8\mathrm{M}_\odot$. The corresponding supernova rate was of $0.045\,\mathrm{yr}^{-1}$, which corresponds to about 1 SN event every 22 yr. Therefore, we find that a rather modest (both in time and intensity) starburst scenario is able to satisfactorily account for both the observed far infra-red and radio luminosity of NGC 5033. (Interestingly, NGC 5033 has been host galaxy to at least three supernovae in the last 60 yr: SN 1950C, SN 1985L, and SN 2001gd, although the supernova rate we have inferred applies for the nuclear and circumnuclear regions, where the main bulk of radio and FIR emission come.)

4.3 The nature of the non-nuclear radio sources in NGC 5033

We now discuss the nature of the four sources (N1, SW1, SW2, and E1; see Table 1) detected in the VLA images well within the radio contours of the 1.4 GHz VLA-C radio emission (panels (a) and (c) in Fig. 1.

4.3.1 Source N1

N1 is catalogued in Ho & Ulvestad (2001) as a background source. N1 is also detected in our 4.9 and 8.4 GHz images, taken 10 years later than the 1.4 GHz in Fig. 1. (see also Table 1). Its spectral index between 4.9 and 8.4 GHz is $\alpha \approx -1.1$, and if we assume no variability between 1993 and 2003, the integrated spectral index from 1.4 to 8.4 GHz is $\alpha = -0.8 \pm 0.1$. From our 8.4 GHz VLA-D image, which yields the highest resolution, the coordinates of N1 are α=13$^{\mathrm{h}}$13$^{\mathrm{m}}$33$^{\mathrm{s}}$.44$\pm$0$^{\mathrm{s}}$.02, δ=36°37′28″.7$\pm$0″.2 (J2000.0), These coordinates are coincident with those reported for FIRST J131333.4+363728 (Becker et al. 1995), which suggests N1 being a background source. Moreover, N1 is about 6″ away from the closest H II regions, so it is likely to be unrelated to them. We therefore conclude that N1 is a background source.

4.3.2 Source SW1

SW1 had a 1.4 GHz peak flux density of 4.5 mJy on April 1993, and was also detected at 4.9 GHz and 8.4 GHz (peaks of 0.66 mJy and 0.36 mJy, respectively). The source was tentatively identified as a background source by Ho & Ulvestad (2001), at a flux density level of 0.3 mJy at 4.9 GHz. The source therefore shows some variability, but the up-and-down behaviour at 4.9 GHz is at odds with it being a radio supernova. The closest H II region is about 5″away from the radio position (Evans 1996), which suggests it is unrelated to it. Finally, the source was detected by ROSAT, but there is no detection in the optical. We therefore suggest, as previous authors, that SW1 is also a background source.

4.3.3 Source E1

E1, detected in our 8.4 GHz VLA-D observations (panel (c) in Figure 1), also coincides with the source J131330.1+363537 detected by Ho & Ulvestad (2001) with a flux density of $S_{4.9} \approx 0.20 \pm 0.06$ mJy, and which these authors tentatively identified as a background source. Our continuum 8.4 GHz radio observations indicate an angular size for E1 of $\simeq 7.4''$(corresponding to a linear size of $\simeq$ 470 pc). The 8.4 GHz flux density of above $2\,\sigma$ is $S_{8.4} = (123 \pm 19)\mu$Jy. We also used *XMM-Newton* archival data of NGC 5033 taken on 18 December 2002 as part of an observing program to observe SN 2001gd, and refer the reader to Pérez-Torres et al (2005) for further technical details. We analyzed the X-ray data in a region ofz 9″in radius (approximately the same size as the radio emitting region), and centered at the peak of 8.4 GHz radio emission. The X-ray spectrum has 200$\pm$20 counts, and is best fit by an optically thin thermal plasma with temperature $kT = 2.3^{+1.6}_{-0.6}$ keV and column density $N_{\mathrm{H}} = (1.8^{+1.3}_{-0.8}) \times 10^{21}$ cm^{-2}, for a galactic column density of $N_{\mathrm{H}}^{\mathrm{gal}} = 1.1 \times 10^{20}$ cm^{-2}.

For the reasons outlined in the previous paragraph, we suggest that E1 is a radio "spur" which emanates from the disk of NGC 5033. Such radio spurs can be observed as a consequence of the formation of superbubbles of size $\sim 300 - 1000$ pc, if sequential Type II supernovae explosions occur every $\sim 10^5$ yr during the lifetime of a giant molecular cloud, canonically taken to be $\sim 1 - 2 \times 10^7$ yr (Norman & Ikeuchi 1989 and references therein) and have been previously detected, e.g., in NGC 253 (Heesen et al. 2004). The energy input by stellar winds and multiple supernovae resulting from OB associations results in an over-

pressurized region (the bubble), that expands and pops out of the disk. The supernovae explosions would then accelerate the relativistic electrons that, immersed in a magnetic field, would be responsible for the observed synchrotron radio emission, which is observed as a radio spur.

The non-thermal spectral index for the spur, $\alpha_{4.9}^{8.4} \simeq$-0.9, is similar to the non-thermal spectra observed for radio supernovae. If the synchrotron spectrum holds at least between 300 MHz and 30 GHz, the total radio luminosity of the spur would be $1.1\times10^{36}\, D_{13}^2$ ergs s^{-1}, a typical value for relatively old radio supernovae, or young supernova remnants. We can then estimate the minimum total energy in relativistic particles and fields, and the approximate equipartition magnetic field (Eq. 1) in the radio spur from minimum energy arguments (Pacholczyk 1970):

$$E_{\rm min} = c_{13}\,(1+\psi)^{4/7}\,\phi^{3/7}\,R^{9/7}\,L_{\rm R}^{4/7} \qquad (2)$$

where c_{13} is a slowly-varying function of the spectral index, and the rest of the parameters have the same meaning as in Eq. 1, and we will also use $\phi = 0.5$ and $\psi = 100$ for the sake of simplicity.

We then obtain $E_{\rm min} \simeq 4\times10^{52}$ ergs and $B_{\rm min} \simeq 13\,\mu$G. The lifetime of the radio spur can be obtained by assuming that its observed radio luminosity has been constant. In that case, $\tau_{\rm spur} = E_{\rm rel}/L_{\rm R}$. Since the relativistic particle energy is $E_{\rm rel} = 4/7(1+\psi)E_{\rm min} \simeq 4.3\times10^{50}$ ergs, we get $\tau_{\rm spur} \simeq 16.1$ Myr. This value agrees well with the expected lifetime for giant molecular clouds, estimated to be $\sim 10-20$ Myr.

The characteristic lifetime of electrons undergoing radiative synchrotron losses is (see, e.g., Pacholczyk 1970)

$$\tau_{\rm syn} = \frac{E}{-(dE/dt)_{\rm syn}} \simeq 33.4\,B_{10}^{-3/2}\,\nu_1^{-1/2}\,{\rm Myr} \qquad (3)$$

where B_{10} is the magnetic field in units of 10μG, and ν_1 is the critical frequency, in GHz. Hence, the non-thermal electrons emitted in the radio spur have lifetimes of about 19.0, 8.6, and 6.6 Myr at 1.4, 4.9, and 8.4 GHz, respectively. It then follows that while the low-frequency radio emission (1.4 GHz) of the radio spur may be due to synchrotron losses of the initially injected electron population, the higher frequency radio emission requires either subsequent injection of fresh electrons, or a reacceleration of the old ones, or both. These facts are all in agreement with the cosmic ray electrons in the radio spur being injected by young supernovae and supernovae remnants occurring during the lifetime of the host giant molecular cloud.

In summary, while we cannot completely exclude that N1 is a background radio source, there is huge evidence for it being a galactic source, namely a radio spur. Indeed, the size ($\simeq$ 470 pc), radio spectrum ($\alpha \simeq -0.9$), high temperature of the ionized plasma ($T_{\rm e} \simeq 2.5\times10^7$ K), and radiative lifetime of the putative spur ($\simeq$ 16 Myr) suggest that it could be a hot superbubble formed as a consequence of sequential supernova explosions occurring during the lifetime of a giant molecular cloud.

4.3.4 Source SW2

SW2 was detected at 1.4 GHz in August 1993 ($S_{1.4}^P$ = 1.85 mJy beam^{-1}), and further identified at 4.9 GHz in April 2003 ($S_{4.9}^P$ = 0.32 mJy beam^{-1}). The radio location of SW2 is spatially coincident, within less than 1.5″, with an H II region of NGC 5033 (Evans 1996) and an optical counterpart from the NOMAD catalogue (Zacharias et al. 2004) (observed in 1963 with $B = 19.64$ and $R = 19.97$). In turn, this H II region is close to a region detected with the WFPC2 camera onboard HST, which suggests their emission is physically related. Thus, SW2 would appear to be of galactic origin. A possible scenario could be that proposed for E1 in the previous paragraphs, i.e., that SW2 is a radio spur. The angular size of the spur, about 8″in radius (≈500 pc) is a typical value for the putative superbubble. An alternative (galactic) scenario could be that of a radio supernova that exploded around 1993. The observed 1.4 GHz luminosity would then correspond to an event about three times fainter than SN 2001gd at its peak. However, both the radio spur and the radio supernova scenarios are very difficult to reconcile with the fact that we did not detect any 8.4 GHz emission on April 2003 above 57μJy (3 σ) around the position of SW2, which implies a very steep spectrum $\alpha_{4.9}^{8.4} \approx -3.0$, and which rather suggests an extragalactic origin for this source. In sum, while it would seem that SW2 belongs to NGC 5033, we cannot rule out the possibility that this is a background source.

5 SUMMARY

We have presented continuum VLA observations of the Sy 1.5 galaxy NGC 5033, made at 4.9 and 8.4 GHz on 8 April 2003, and also archival VLA data at 1.4 and 4.9 GHz, which probe the radio emission of this galaxy from regions of less than a hundred parsecs up to more than 35 kpc in size. We summarize our main results as follows:

- The high-resolution VLA images show a core-jet structure for the Sy 1.5 nucleus. The core has a moderately steep radio spectrum, ($S_\nu \propto \nu^\alpha$; $\alpha_{1.5}^{4.9} = -0.44\pm0.04$). The 1.4 GHz radio emission, as traced by the VLA in C configuration, correlates very well with the optical emission of the whole galaxy, and delineates exquisitely the spiral arms. Our 4.9 and 8.4 GHz simultaneous observations with the VLA-D show only significant radio emission from the inner disk of the galaxy. Combining the data at 1.4, 4.9, and 8.4 GHz, we find that the radio emission of the inner disk of the galaxy shows a steep spectrum ($\alpha_{1.4}^{8.4} \approx -0.9$), which is usually found in galaxies where radiative losses are high in the disk of the galaxy, so that the escape rate of their cosmic ray electrons is low (Lisenfeld & Voelk 2000).
- If the synchrotron spectrum extends at least from 300 MHz to 30 GHz, the isotropic radio luminosity of the inner disk of NGC 5033 is $L_{\rm R}(2.9 \pm 0.3) \times 10^{21}\, D_{13}^2$ W m^{-2} Hz^{-1}. Combining this value with the far-infrared luminosity of the galaxy ($L_{\rm FIR} = 1.20\times10^{10}L_\odot$), we obtained a value for the q parameter of 2.83, which indicates that the radio emission from the inner regions of NGC 5033 is mainly powered by a recent starburst. In fact, the compact core-jet structure at the center of the galaxy, contributes only about 7% of the total 1.4 GHz radio luminosity. We find that a relatively short starburst, lasting 10 Myr and and producing stars at a rate of 2.8 M$_\odot$ yr^{-1} in the range $m_l = 1$ M$_\odot$ and $m_u = 40$ M$_\odot$, reproduces very well the observed radio and far-infrared luminosities, and

results into a supernova rate of $0.045\,\mathrm{yr}^{-1}$. This supernova rate corresponds to about 1 SN event every 22 yr.

- We find evidence for the existence of a radio "spur" (E1) of radius $r \simeq 470$ pc, located at a distance of about 2.1 kpc above the disk plane. Its radio spectrum ($\alpha \simeq -1.1$), high temperature of the ionized plasma ($T_{\rm e} \simeq 2.5 \times 10^7$ K), and lifetime ($\tau \simeq 16$ Myr) strongly suggest that it is a hot superbubble formed as a consequence of sequential supernova explosions occurring during the lifetime of a giant molecular cloud.

ACKNOWLEDGMENTS

We thank the referee, Marek Kukula, for his comments and careful reading of the manuscript. We also thank Martín Guerrero for helping us with the X-ray calculations, and to Enrique Pérez for helpful discussions. This research was partially funded by grants AYA2005-08561-C03-02 and AYA2002-00897 of the Spanish Ministerio de Ciencia y Tecnología. MAPT is supported by the Spanish National programme Ramón y Cajal. NRAO is a facility of the USA National Science Foundation operated under cooperative agreement by Associated Universities, Inc. We made extensive use of the NASA Astrophysics Data System Abstract Service and of the Aladin (v4.006) software, developed and maintained by the Centre de Données Astronomiques de Strasbourg (CDS).

REFERENCES

Becker R. H., White R. L. & Helfand D. J., 1995, A&A, 450, 559
Carilli C. L., Holdaway M. A., Ho P. T., De Pree C. G., 1992, ApJ, 399, L59
Colla G. et al., 1973, A&AS, 11, 291
Condon J. J., Anderson M. L., & Helou G., 1991, ApJ, 376, 95
Condon J. J., Huang Z. P., Yin Q. F., & Thuan, T. X. 1991b, ApJ, 378, 65
Condon J. J., 1992, ARA&A, 30, 575
De Breuck C., van Breugel W., Röttgering H. J. A., Miley G., 2000, A&AS, 143, 303
Falco E. E., et al., Updated Zwicky Catalog (UZC), 1999, PASP, 111, 438
Evans I. N., Koratkar A. P., Storchi-Bergmann T., Kirkpatrick H., Heckman T. M., Wilson A. S., 1996, ApJS, 105, 93
Harwit M., & Pacini F. 1975, ApJ, 200, L127
Heesen V., Krause M., Beck R., & Dettmar R.-J., 2004, Proceedings of The Magnetized Plasma in Galaxy Evolution, 156, Eds. Chyzy, K., Otmianowska-Mazur, K., Soida, M., & Dettmar, R.-J.,
Hales S. E. G., Baldwin J. E. & Warner P. J., 1988, MNRAS, 234, 919
Helou G., Soifer B. T. & Rowan-Robinson M., 1985, ApJ, 298, L7
Ho L. C., Filippenko A. V., Sargent W. L. W., 1997, ApJS, 112, 315
Ho L. C. & Ulvestad J., 2001, ApJS, 133, 77
Izvekova V. A., Kuzmin A. D., Malofeev V. M., Shitov Y. P., 1981, Ap&SS, 78, 45
Laing R. A., Bridle A. H., 2002, MNRAS, 336, 328
Lisenfeld U., Alexander P., Pooley G. G., Wilding T., 1996, MNRAS, 281, 301
Lisenfeld U. & Voelk H. J., 2000, A&A, 354, 423
McMahon R. G., White R. L., Helfand D. J., Becker R. H., 2002, ApJS, 143, 1
Moffet A. T., in Galaxies and the Universe, 1973, Vol. 9, Chap. 7. Sandage A. Sandage M., Kristian J. (eds.), Univ. Chicago Press
Norman C. A. & Ikeuchi S., 1989, ApJ, 345, 372
Pacholczyk A. G., 1970, Radio Astrophysics (San Francisco: Freeman)
Pacholczyk A. G., 1977, Radio Galaxies (Oxford: Pergamon Press)
Pérez-Torres M. A., et al., 2005, MNRAS, 360, 1055
Sanders D. B. & Mirabel I. F., 1996, ARA&A, 34, 749
Sanders D. B., Mazzarella J. M., Kim D.-C., Surace J. A., Soifer B. T. 2003, AJ, 126, 1607
Scoville N. Z., Yun M. S., Bryant P. M., 1997, ApJ, 484, 702
Seaquist E.R. & Odegard N., 1991, ApJ, 369, 320
Sukumar S., Velusamy T. & Klein U., 1988, MNRAS, 231, 765
Yun M. S., Reddy N. A. & Condon, J. J., 2001, ApJ, 554, 803
Zacharias N., Urban S. E., Zacharias M. I., Wycoff G. L., Hall D. M., Monet D. G., Rafferty T. J., 2004, AJ, 127, 3043

This paper has been typeset from a TEX/ LATEX file prepared by the author.